Volume 44 | Number 24 | 28 June 2015 | Pages 10891–11242

Dalton Transactions

An international journal of inorganic chemistry

www.rsc.org/dalton

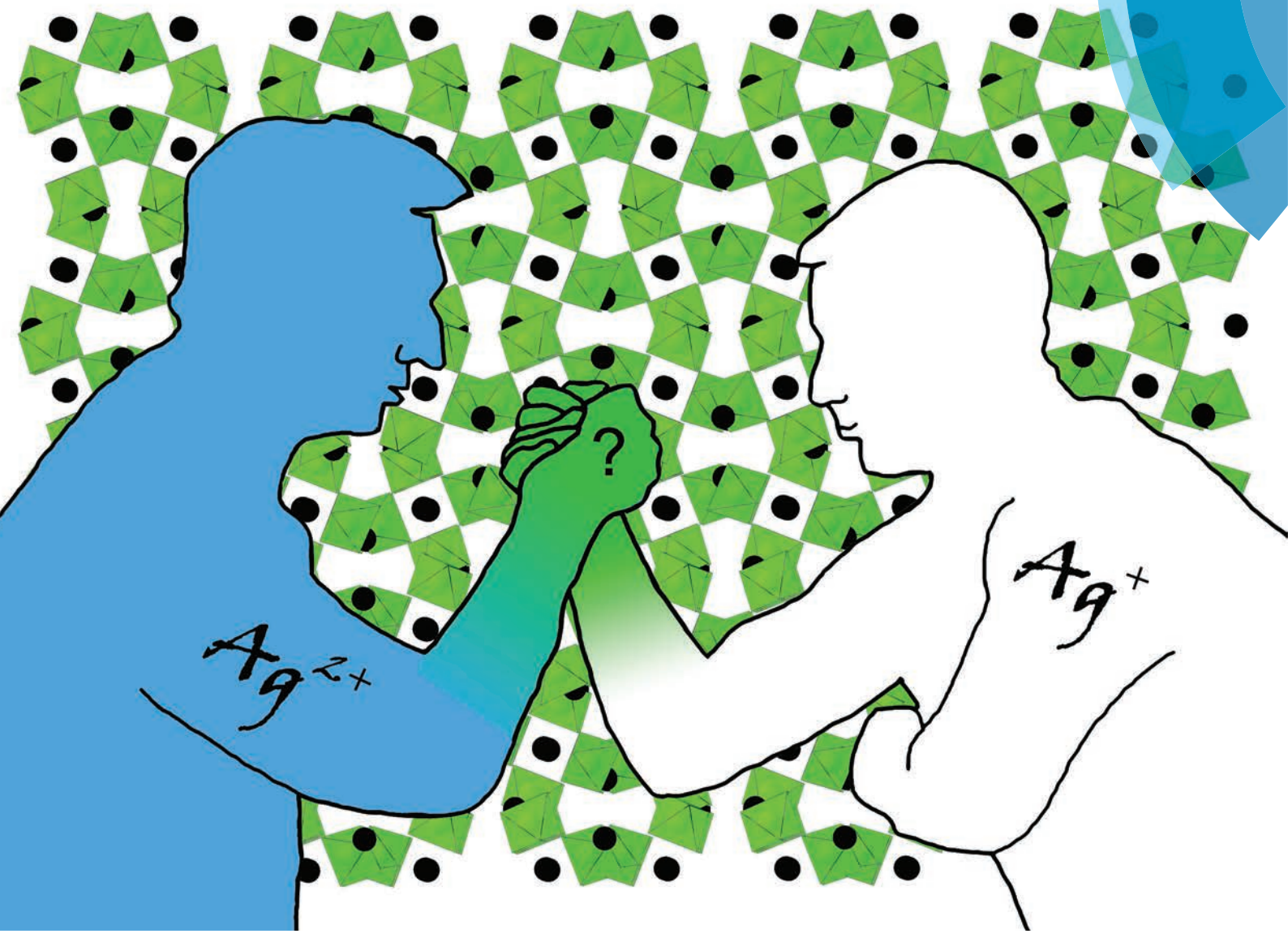

ISSN 1477-9226

ROYAL SOCIETY OF CHEMISTRY

PAPER

Zoran Mazej, Wojciech Grochala *et al.*

The first example of a mixed valence ternary compound of silver with random distribution of Ag(I) and Ag(II) cations

Dalton Transactions

PAPER

View Article Online
View Journal | View Issue

Cite this: *Dalton Trans.*, 2015, **44**, 10957

The first example of a mixed valence ternary compound of silver with random distribution of Ag(I) and Ag(II) cations†

Zoran Mazej,*[a] Tomasz Michałowski,[b,c] Evgeny A. Goreshnik,[a] Zvonko Jagličić,[d] Iztok Arčon,[e,f] Jadwiga Szydłowska[c] and Wojciech Grochala*[b]

Received 19th February 2015,
Accepted 18th March 2015

DOI: 10.1039/c5dt00740b

www.rsc.org/dalton

The reaction between colourless $AgSbF_6$ and sky-blue $Ag(SbF_6)_2$ (molar ratio 2 : 1) in gaseous HF at 323 K yields green $Ag_3(SbF_6)_4$, a new mixed-valence ternary fluoride of silver. Unlike in all other Ag(I)/Ag(II) systems known to date, the Ag^+ and Ag^{2+} cations are randomly distributed on a single 12b Wyckoff position at the $\bar{4}$ axis of the $I\bar{4}3d$ cell. Each silver forms four short (4 × 2.316(7) Å) and four long (4 × 2.764(6) Å) contacts with the neighbouring fluorine atoms. The valence bond sum analysis suggests that such coordination would correspond to a severely overbonded Ag(I) and strongly underbonded Ag(II). Thorough inspection of thermal ellipsoids of the fluorine atoms closest to Ag centres reveals their unusual shape, indicating that silver atoms must in fact have different local coordination spheres; this is not immediately apparent from the crystal structure due to static disorder of fluorine atoms. The Ag K-edge XANES analysis confirmed that the average oxidation state of silver is indeed close to $+1\frac{1}{3}$. The optical absorption spectra lack features typical of a metal thus pointing out to the semiconducting nature of $Ag_3(SbF_6)_4$. $Ag_3(SbF_6)_4$ is magnetically diluted and paramagnetic (μ_{eff} = 1.9 μ_B) down to 20 K with a very weak temperature independent paramagnetism. Below 20 K weak antiferromagnetism is observed (Θ = −4.1 K). Replacement of Ag(I) with potassium gives $K(I)_2Ag(II)(SbF_6)_4$ which is isostructural to $Ag(I)_2Ag(II)(SbF_6)_4$. $Ag_3(SbF_6)_4$ is a genuine mixed-valence Ag(I)/Ag(II) compound, *i.e.* Robin and Day Class I system (localized valences), despite Ag(I) and Ag(II) adopting the same crystallographic position.

Introduction

Chemical compounds with an element in more than one oxidation state have been labelled as "mixed-valence" systems, although the expression "mixed oxidation state compounds" perhaps conveys a clearer idea about what is signified.[1–3] One striking feature about many mixed-valence compounds is their intense colour; some – such as minium ($Pb(II)_2Pb(IV)O_4$), or magnetite ($Fe(II)Fe(III)_2O_4$) – have been used since antiquity as pigments. Prussian blue, $Fe(III)_4[Fe(II)(CN)_6]_3{\cdot}nH_2O$, first prepared over three centuries ago well before the organic chemists joined the dye business, was the first mixed-valence inorganic compound synthesized by men for use in paints and inks.[4] In 1967 Robin and Day[5] (almost simultaneously with Allen and Hush[6]) published an extensive survey of mixed-valence systems. Their classification, which remains widely utilized today, is based upon the local symmetry and strength of the ligand fields around metal cations. In Class I systems, cations are found in sites of different symmetry and/or ligand field strength (valences are firmly trapped, *i.e.* localized; such compounds adopt mixed valence). On the other hand, in Class III the electron density is delocalized over cationic sites and two

[a]*Department of Inorganic Chemistry and Technology, Jožef Stefan Institute, Jamova 39, SI–1000 Ljubljana, Slovenia. E-mail: zoran.mazej@ijs.si*
[b]*CENT, University of Warsaw, Żwirki i Wigury 93, 02–089 Warsaw, Poland. E-mail: w.grochala@cent.uw.edu.pl*
[c]*Faculty of Chemistry, University of Warsaw, Pasteur 1, 02–093 Warsaw, Poland*
[d]*University of Ljubljana, Faculty of Civil and Geodetic Engineering, and Institute of Mathematics, Physics and Mechanics, Jadranska 19, SI–1000 Ljubljana, Slovenia*
[e]*University of Nova Gorica, Vipavska 13, SI–5000 Nova Gorica, Slovenia*
[f]*Department of Low and Medium Energy Physics, Jožef Stefan Institute, Jamova 39, SI–1000 Ljubljana, Slovenia*

†Electronic supplementary information (ESI) available: X-ray crystallographic files in the CIF format, a photo of a $Ag(SbF_6)_2$ solution in aHF, the Raman spectrum of impure blue-green $Ag(SbF_6)_2$, photos showing self-supported homogeneous pellets used for XANES spectroscopy, XRDP for a powder sample of $Ag_3(SbF_6)_4$, Raman spectra of $Ag_3(SbF_6)_4$ compared to several relevant reference samples, FIR and MIR absorption spectra for $Ag_3(SbF_6)_4$, $Ag(SbF_6)_2$, and $AgSbF_6$, comparison of magnetic properties of $Ag_3(SbF_6)_4$ and $Ag(SbF_6)_2$, M *vs.* H curves at various temperatures for $Ag(SbF_6)_2$, and NUV absorption spectra for $Ag_3(SbF_6)_4$, $Ag(SbF_6)_2$ and $AgSbF_6$. Further details of the crystal structure determination could be found and CIF files may be obtained from Fachinformationszentrum Karlsruhe, 76344 Eggenstein-Leopoldshafen, Germany (e-mail: crysdata@fiz-karlsruhe.de; http://www.fiz-karlsruhe.de/request_for_deposited_data.html). CCDC 429207 ($Ag_3(SbF_6)_4$) and 429208 ($K_2Ag(SbF_6)_4$). For ESI and crystallographic data in CIF or other electronic format see DOI: 10.1039/c5dt00740b

distinct oxidation states cannot be distinguished ("intermediate valence") – such systems often exhibit metallic conductivity. In some cases it is not possible to make a clear demarcation between Class I and Class III behaviour. Class II compounds represent such a rare intermediate case in which some degree of delocalization is observed although the cationic sites remain distinguishable. One of the most famous examples of Class II systems is the so called Creutz–Taube Ru(II)/Ru(III) complex,[7] which reveals Class I or Class III characteristics depending on the energy/time scale of experiments ("dynamic delocalization").

Mixed-valence compounds exhibit a broad range of fascinating physicochemical properties which are related to electron transfer between distinct oxidation states (*i.e.* intervalence charge transfer).[8] The most striking of those is high-temperature superconductivity which results from either hole or electron doping to layered Cu(II) oxides[9,10] to an appropriate degree;[11,12] doping may be realized either *via* chemical substitutions or charge injection[13,14] formally leading to introduction of Cu(III) or Cu(I) to the parent Cu(II) systems. Chemically doped copper oxides are now the best crystallographically researched group of inorganic compounds, with over eight thousand distinct structures available in databases.[15] In majority of cases (except for YBCO-like systems) these are Class III systems, where doped charge is equally distributed over all copper sites.

Silver is a heavier sibling of copper and it is natural to search for superconductivity in doped compounds of Ag(II). Many such attempts were made in the early days of oxocuprate superconductivity[16] (late 1980s–early 1990s) but without success – in each case only Ag(I) could be introduced into the oxide matrix, which was detrimental to superconducting properties. Only later it was realized that the oxide environment is not appropriate for hosting paramagnetic Ag(II) since the latter species is an enormously strong oxidizer (thus it cannot be obtained by the action of O_2, and it is readily reduced to Ag(I)[17]) and it also tends to disproportionate to Ag(I) and Ag(III) in the oxide environment.[18,19] Instead, Ag(II) systems with fluoride anions were suggested as being analogous to Cu(II) oxides as evidenced by many similarities between the two families of compounds. Moreover, the quantum mechanical calculations have revealed that layered Ag(II) fluorides would have a strikingly similar electronic structure to that of undoped oxocuprates,[20,21] thus supporting the surmise that superconductivity could be generated upon doping to the former type of material just like it is observed for the latter.[22]

Regretfully, mixed-valence compounds of silver are quite rare, with about 20 documented stoichiometries (*cf.* Table 1 in ref. 23). The Ag(II)/Ag(I) system – relevant to electron doping to the parent Ag(II) compound – is limited to two complex compounds with organic ligands,[24–26] and two inorganic systems: $Ag_3(SO_3F)_4$ [27,28] and a recently prepared $Ag_9(PO_2F_2)_{14}$.[29,30] The first coordination spheres of Ag(I) and Ag(II) in these systems are quite different: in organic systems both types of silver cations are coordinated by different ligands, while in homoleptic inorganic systems Ag(II) and Ag(I) sit on different crystallographic sites and the local geometries around them differ markedly, thus leading in all cases to the Class I behaviour.

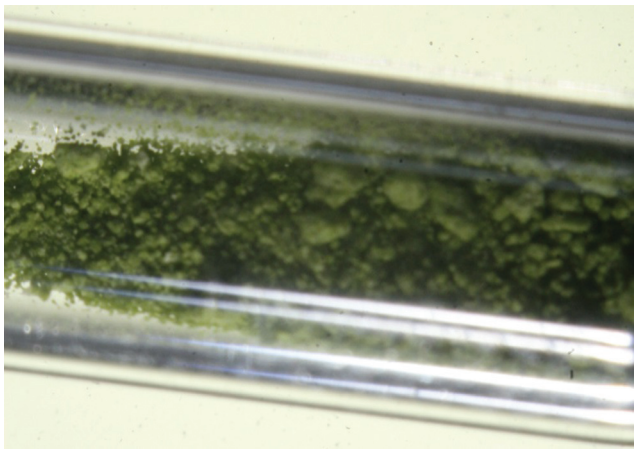

Fig. 1 A sample of extremely moisture-sensitive green $Ag(I)_2Ag(II)(SbF_6)_4$ enclosed in a prefluorinated 0.3 mm quartz capillary.

In the present work, we describe the results of detailed examination of green $Ag_3(SbF_6)_4$ (Fig. 1) and of a related $K_2Ag(SbF_6)_4$. We show that $Ag_3(SbF_6)_4$ – unlike its predecessors – is an example of a mixed valence ternary compound of silver ($Ag(I)_2Ag(II)(SbF_6)_4$) with random distribution of Ag(I) and Ag(II) cations on the same crystallographic site in the crystal lattice – which nevertheless preserves a localized-valence character – and we discuss possible consequences of this finding.

Experimental

Caution: anhydrous HF (aHF) and some fluorides are highly toxic and must be handled using appropriate apparatus and protective gear. Organic matter may ignite upon contact with compounds of Ag(II).[31]

Materials and methods

Reagents. $AgNO_3$ (Alkaloid Skopje, 99.7%) and BF_3 (Union Carbide Austria GmbH, 99.5%) were used as supplied. $AgBF_4$, $AgSbF_6$, $AgSb_2F_{11}$ and $IF_6[Ag(SbF_6)_3]$ were prepared by methods as described in the literature.[32,33] AgF_2 was obtained by fluorination of $AgNO_3$ in aHF, meanwhile a SbF_5–HF mixture was prepared by fluorination of SbF_3 in aHF. Pure SbF_5 was prepared by fluorination of SbF_3 in a flow reaction, and its purity was checked by Raman spectroscopy. $Ag(SbF_6)_2$ was prepared from AgF_2 and a SbF_5–HF mixture as described previous1y.[34] A freshly prepared $Ag(SbF_6)_2$ should be sky-blue without any traces of green particles as observed in some reactions (*cf.* ESI†).

Synthetic apparatus. Volatile materials (SbF_5, aHF) were handled in an all-PTFE vacuum line equipped with PTFE valves. The manipulation of the non-volatile materials sensitive to moisture was done in a glovebox (M. Braun). The residual water in the atmosphere within the dry box never exceeded

1 ppm. The reactions were carried out in FEP (tetrafluoroethylene–hexafluoropropylene) reaction vessels (length 250–300 mm, i.d. 16 mm, o.d. 19 mm) equipped with PTFE valves and PTFE coated stirring bars. Prior to use, all reaction vessels were passivated with elemental fluorine. Fluorine was used as supplied (Solvay, Germany). Anhydrous HF (Linde, 99.995%) was treated with K_2NiF_6 (Advance Research Chemicals, Inc.) for several hours prior to use.

Synthetic procedures

Reaction between $AgSbF_6$ and $Ag(SbF_6)_2$ in liquid aHF. A mixture of $AgSbF_6$ (0.62 mmol, 214 mg) and $Ag(SbF_6)_2$ (0.31 mmol, 180 mg) was loaded in a reaction vessel in a dry box. Anhydrous HF (4 mL) was condensed onto the reaction mixture and the reaction vessel was warmed to ambient temperature. Since some white insoluble solid was still visible, additional 4 ml of aHF were added. After warming the reaction mixture to ambient temperature, a light blue solution was obtained. After one day of intense stirring, the volatiles were pumped off at ambient temperature. The final mass of the isolated green solid was 0.390 mg (calcd for $Ag_3(SbF_6)_4$: 0.394 mg). Raman spectra and X-ray powder diffraction patterns of the remaining solid showed not only the presence of $Ag_3(SbF_6)_4$ but also the presence of the starting $AgSbF_6$ and $Ag(SbF_6)_2$.

Reaction between $AgSbF_6$ and $Ag(SbF_6)_2$ in liquid SbF_5. $AgSbF_6$ (0.48 mmol, 165 mg) and $Ag(SbF_6)_2$ (0.24 mmol, 139 mg) were loaded in a glovebox into the FEP reaction vessel. Then SbF_5 (~2 ml) was condensed on it at 77 K and the mixture was warmed up to room temperature. The reaction was left to proceed for one day. Since there was no visible change (only bluish insoluble stuff was observed) and the reaction mixture was very viscous, a small amount of gaseous aHF was added to decrease the viscosity of the liquid phase. After an additional day no change had been observed.

Reaction between $AgSb_2F_{11}$ and AgF_2 in gaseous HF. 0.070 g (0.24 mmol) of dark brown AgF_2 and 0.538 mg of colourless $AgSb_2F_{11}$ (0.48 mmol) were loaded in a dry-box into a 35 ml FEP reaction vessel. aHF was added at room temperature till the final pressure in the reaction vessel reached 0.93 bar. The brown reaction mixture immediately turned to olive green. After one day, volatiles were pumped off at room temperature. The Raman spectrum of the isolated green solid showed the presence of starting materials and $Ag_3(SbF_6)_4$. Since the inspection under a microscope showed the presence of dark particles, the treatment with gaseous aHF was repeated. The Raman spectrum of the isolated green solid showed the presence of $AgSbF_6$ and $Ag_3(SbF_6)_4$, meanwhile inspection under the microscope showed the presence of a predominantly green solid with some blue particles. Attempts to obtain X-ray powder diffraction patterns were unsuccessful.

Reduction of $Ag(SbF_6)_2$, dissolved in aHF, by elemental hydrogen. In the first experiment 0.215 g (1.48 mmol) of AgF_2 was loaded in a glovebox into an FEP reaction vessel and 0.98 g (4.52 mmol) SbF_5 and aHF (6 ml) were condensed on it at 77 K. The reaction vessel was brought up to 298 K and a clear blue solution formed in a few minutes. Hydrogen was added to the final pressure of 4 bar. The blue solution changed its colour to green immediately after the addition of hydrogen. In a few minutes a white solid started to precipitate and the solution became colourless. After volatiles were pumped off at room temperature 0.680 g of white solid was obtained. The Raman spectrum showed the mixture of $AgSbF_6$ and $AgSb_2F_{11}$. In the second experiment 0.855 g (1.41 mmol) $Ag(SbF_6)_2$ was dissolved in 6 ml of aHF. The reaction vessel was brought up to 298 K and a clear blue solution formed. After small addition of hydrogen a white solid started to precipitate, meanwhile the solution remained blue.

Reaction between $Ag(SbF_6)_2$ and H_2O in liquid aHF. 0.815 g (1.41 mmol) of $Ag(SbF_6)_2$ was loaded in a glovebox into an FEP reaction vessel. Then aHF (4 ml) was condensed on the reaction mixture at 77 K and 0.025 g (1.41 mmol) of water was added. The reaction vessel was warmed to ambient temperature. A clear blue solution formed above the white precipitate. Volatiles were pumped away at ambient temperature. The Raman spectrum was in agreement with literature data for $AgSbF_6$ and $Ag(SbF_6)_2$.

Synthesis of high-purity $Ag_3(SbF_6)_4$. In a glovebox 2.28 mmol (0.784 g) of $AgSbF_6$ and 1.14 mmol (0.661 g) of $Ag(SbF_6)_2$ were loaded into a FEP tube (V = 8 ml, 6 mm o.d.). aHF was added at room temperature till the final pressure in the tube reached 0.93 bar. Immediately after the first traces of aHF were added to the bluish $AgSbF_6$–$Ag(SbF_6)_2$ mixture, its colour changed from blue to olive green. The bottom of the FEP tube containing the $AgSbF_6$–$Ag(SbF_6)_2$ mixture was cooled down to 77 K. After aHF condensed at the bottom, the upper part of the FEP tube was sealed using the small flame of a gas burner using flat-nose pliers. A sealed tube was taken in a dry-box and placed inside a larger glass tube with a ground glass neck. The glass tube was closed with a glass valve. In that way, the FEP tube with the $AgSbF_6$–$Ag(SbF_6)_2$–aHF reaction mixture was surrounded by an inert atmosphere which was preventing the diffusion of moisture from the atmosphere to the reaction mixture through walls of the FEP tube (an attempt without using the glass tube filled with argon resulted in complete reduction of Ag(II) and formation of $AgSbF_6$/$AgSb_2F_{11}$). An additional reason for selecting the glass instead of, for example, a metal tube was the possibility to monitor the colour of the solid inside the FEP tube. A glass tube was connected to a vacuum system and a small amount of argon was pumped away. Only 0.6 bar were left inside. A closed glass tube containing a sealed FEP tube was heated up to 318 K. After two days the glass tube was cooled down and transferred inside the dry-box where it was opened. A small FEP tube was cut and quickly transferred into a larger FEP reaction vessel. Outside the glovebox the FEP reaction vessel containing the opened FEP tube was connected to a vacuum system and Ar and aHF were pumped away over the night. After that the sample was first finely ground in an agate mortar inside the dry-box and then placed into a new FEP tube. The whole procedure of adding aHF, sealing, *etc*. has been repeated. Reaction at 318 K

was left to proceed for one day and isolation was done as described previously. An olive green solid was isolated. A very homogeneous olive-green solid was observed under a microscope without any blue particles which could be attributed to $Ag(SbF_6)_2$. The X-ray powder diffraction pattern of the olive green $Ag_3(SbF_6)_4$ powder obtained by syntheses was the same as the X-ray powder diffraction pattern calculated from the crystal structure of $Ag_3(SbF_6)_4$. In addition, the Raman spectra of the bulk material and of the single crystal of $Ag_3(SbF_6)_4$ were virtually identical.

There are two crucial factors which may impact the fate of this reaction. The first one is the amount of aHF; if it is too large and sufficient that aHF will start to liquefy when the reactor is cooled down to ambient temperature, $aHF_{(l)}$ will inevitably solvolize part of the $Ag_3(SbF_6)_4$ product back to $AgSbF_6$ and $Ag(SbF_6)_2$ which is detected as blue staining of the liquid phase. The second important thing is to avoid the diffusion of traces of water and even oxygen through the walls of the FEP tube which could lead to reduction of Ag(II).

Crystallography

Growth of single crystals of $Ag_3(SbF_6)_4$ and $K_2Ag(SbF_6)_4$. Single crystal growth was carried out in double T-shaped apparatus consisting of two FEP tubes (19 mm o.d., and 6 mm o.d.). Around 300 mg $Ag(SbF_6)_2$ was loaded into the wider arm of the crystallization vessel in a dry-box. aHF (~6 mL) was then condensed onto the starting material at 77 K. The crystallization mixtures were brought up to ambient temperature and the clear blue solution, which had developed, was decanted into the narrower arm. The evaporation of the solvent from this solution was carried out by maintaining a temperature gradient corresponding to about 10 °C between both tubes for 10 days. The effect of this treatment was to enable aHF to be slowly evaporated from a narrower into a wider tube leaving the green crystals of $Ag_3(SbF_6)_4$ and some colourless powdered solids. Selected single crystals of $Ag_3(SbF_6)_4$ and colourless particles were placed inside 0.3 mm quartz capillaries in a dry-box and their Raman spectra were recorded. Raman spectra of white particles show a narrow very intense band at 1864 cm^{-1}, characteristic of the presence of the O_2^+ cation (*i.e.* O_2SbF_6).

$KSbF_6$ (0.34 mmol) and $Ag(SbF_6)_2$ (0.17 mmol) were loaded into the 19 mm o.d. arm of the crystallization vessel inside a dry-box. The reagent mixture was then transferred to a metal/Teflon manifold where aHF (5 ml) was condensed onto the starting material at −196 °C. The crystallization mixture was warmed to ambient temperature and the resulting clear, blue solution was decanted into the 6 mm o.d. side arm. Evaporation of the solvent from this solution was carried out by maintaining a temperature gradient of *ca.* 10 °C between the 6 mm o.d. tube and the 19 mm o.d. tube for one day. Slow distillation of aHF from the 6 mm o.d. tube into the 19 mm o.d. tube resulted in crystal growth inside the 6 mm o.d. tube. Selected green single crystals were transferred to 0.3 mm quartz capillaries inside the dry box. In addition, some colorless crystals were observed; their Raman spectra correspond to $KSbF_6$.

Crystal structure determination of $Ag_3(SbF_6)_4$ and $K_2Ag(SbF_6)_4$. Single crystals were immersed in perfluorinated oil (perfluorodecalin, ABCR, 98%) in a dry box, selected under a microscope, and transferred into the cold nitrogen stream of the diffractometer. Data for $Ag_3(SbF_6)_4$ were collected at 150 K on an Agilent Gemini A diffractometer with an Atlas CCD detector, and data for $K_3(SbF_6)_4$ were collected at 200 K on a Rigaku AFC7 diffractometer equipped with a Mercury CCD detector (both using graphite-monochromated Mo-Kα radiation, λ = 0.71069 Å). A multi-scan absorption correction has been applied for both datasets. The structures were solved by direct methods using the SIR-92[35] software (implemented in program packages TeXsan[36] and WinGX,[37] respectively) and refined with SHELXL-97[38] software. The figures were prepared using the DIAMOND 3.1 program.[39]

The corresponding crystal data and refinement results are summarized in Table 1.

Powder X-ray diffraction analysis of $Ag_3(SbF_6)_4$. Powder X-ray diffraction patterns were obtained using a D8 discover diffractometer from Bruker equipped with a Cu-cathode and parallel beam setting provided by Göbel mirrors. The sample was loaded into a thin (0.3 mm diameter, 0.01 mm thick walls) quartz capillary (Hilgenberg) in a dry-box. The obtained powder pattern was analysed using the previously published crystal structures of $AgSbF_6$, $Ag(SbF_6)_2$ and $Ag_3(SbF_6)_4$ (this work). The Reflex QPA module of Materials Studio package[40] gave the following results of quantitative phase analysis: $Ag_3(SbF_6)_4$ 96.6 wt%, $AgSbF_6$ 3.4 wt%, no $Ag(SbF_6)_2$ could be detected (*cf.* ESI†).

Instrumental methods

Raman spectroscopy. Raman spectra were recorded using a Horiba Jobin Yvon LabRam-HR Raman micro-spectrometer with a 632.8 nm He–Ne laser exciting beam. The power of the beam varied from 0.017 mW to 17 mW. Note! The laser power above 1.7 mW leads to photochemical decomposition of $Ag_3(SbF_6)_4$ and formation of $AgSbF_6$. All Raman spectra are shown and discussed in the ESI.†

Magnetic measurements. Magnetic measurements for $Ag_3(SbF_6)_4$ and $Ag(SbF_6)_2$ reference were carried out with a

Table 1 Crystal data and refinement results for $Ag_3(SbF_6)_4$ and $K_2Ag(SbF_6)_4$

Chemical formula	$Ag_3(SbF_6)_4$	$K_2Ag(SbF_6)_4$
F_w (g mol^{-1})	2533.3	2258.1
Space group	$I\bar{4}3d$	$I\bar{4}3d$
a (Å)	12.3613(4)	12.498(1)
V (Å^3)	1888.83(18)	1952.3(4)
Z	4	4
D_{calc} (g cm^{-3})	4.454	3.841
T (K)	150	200
R_1 [a]	0.0297	0.0836
wR_2 [b]	0.0642	0.2055

[a] R_1 is defined as $\sum||F_o| - |F_c||\sum|F_o|$ for $I > 2\sigma(I)$. [b] wR_2 is defined as $[\sum[w(F_o^2 - F_c^2)^2]/\sum w(F_o^2)^2]^{1/2}$ for $I > 2\sigma(I)$.

superconducting quantum interference device magnetometer MPMS-XL-5 from Quantum Design equipped with a 50 kOe magnet, and operating in the temperature range 2–300 K. The measurements were performed in 1 kOe magnetic field. Isothermal magnetization has been measured at several temperatures below 20 K between ±50 kOe (ESI†). The data were corrected for sample holder contribution, a temperature independent magnetic susceptibility of inner shell electrons (Larmor diamagnetism) as obtained from Pascal's tables, and a temperature independent paramagnetism.

ESR spectroscopy. The ESR spectra were obtained with an ESP 300E spectrometer operating at the X-band (frequency 9.5 GHz) from Bruker for samples sealed under an Ar atmosphere inside a 4 mm thick quartz capillary. Measurements were carried out in the temperature interval 120 K–300 K (at 10–15 K increments); only the spectra recorded at the two extreme temperatures are shown. The typical uncertainty of the determination of the components of the *g* tensor is ±0.001.

UV-vis-NIR spectroscopy. The electronic spectra for the samples of $AgSbF_6$, $Ag(SbF_6)_2$ and $Ag_3(SbF_6)_4$ were obtained using a Vertex 80v spectrometer manufactured by Bruker, using transmission mode. Halogen and deuterium lamps were used as the radiation sources with a 2–2.5 mm aperture, a CaF_2 beamsplitter in the optical path, and a RT-Si diode type detector. Powdered samples were loaded under an Ar atmosphere onto one CaF_2 window and assembled, together with another clean CaF_2 window and a separator, as a flat-widow air-tight cuvette used for measurements.

X-ray absorption near-edge structure spectroscopy (XANES). The Ag K-edge XANES spectra of the $Ag(I)_2Ag(II)(SbF_6)_4$ as well as $Ag(I)SbF_6$ and $IF_6[Ag(II)(SbF_6)_3]$ reference compounds were obtained in a standard transmission mode at the BM23 beamline of European Synchrotron Radiation Facility (ESRF) in Grenoble. A Si(311) double-crystal monochromator was used with about 3 eV resolution at 25 514 eV. Harmonics were effectively eliminated by using a flat silicon mirror. The three 30 cm long ionisation chamber was filled with Kr, the first at the pressure of 120 mbar, the second and third at the pressure of 420 mbar.

The absorption spectra were obtained within the −250 eV/+250 eV interval relative to the Ag K-edge. In the XANES region equidistant energy steps of 0.5 eV were used with an integration time of 1 s per step. In all experiments the exact energy calibration was established with simultaneous absorption measurements on a 25 μm thick Ag metal foil placed between the second and the third ionization chamber. The first maximum of the derivative of the Ag foil spectrum was assigned to 25 514.0 eV.

The compounds in the form of fine powder were pressed into self-supported homogeneous pellets (diameter 6 mm, thickness less than 1 mm) in a dry-box to prevent hydrolysis and sealed under an inert atmosphere into a thin-walled FEP tube (*cf.* ESI, Fig. S3†). The FEP tube containing the pellet was mounted on a sample holder in a vacuum chamber of the beam-line. The sealed sample was perfectly stable for several hours of the experiment: no sign of hydrolysis was observed after demounting.

The analysis of Ag K-edge XANES spectra was performed with the IFEFFIT program package ATHENA.[41] The relative Ag K shell contribution in the absorption spectra of the samples was obtained by removing the extrapolated best-fit linear function determined in the pre-edge region (−150 eV to −50 eV). By conventional normalization, extrapolating the post-edge spline background, determined in the range of 50 to 250 eV, the Ag K-edge jump is set to 1.[42–44]

Theoretical methods

Density functional theory (DFT) calculations. DFT calculations were carried out for a primitive cell of $Ag_3(SbF_6)_4$ using the VASP code[45] as available in the Medea package.[15] To describe a hypothetical metallic nature of $Ag_3(SbF_6)_4$ we have used the Generalized Gradient Approximation (GGA) and the PBEsol functional adopted for solids, with the energy cutoff of 500 eV, and *k*-point mesh of 0.2 $Å^{-1}$.

Results and discussion

Towards $Ag_3(SbF_6)_4$ through serendipity and *via* many failures

Solid $Ag(SbF_6)_2$ and its aHF solution have characteristic sky-blue colour typical of the presence of solvated Ag(II) (Fig. S1, ESI†). During the investigations of the Ag(I)/Ag(II)/SbF_5/aHF system in 2003,[33] one of us (ZM) has observed that addition of hydrogen into a clear blue solution of $Ag(SbF_6)_2$ dissolved in aHF–SbF_5, results in the change of colour. The colour of the blue solution first turned to green and with time to colourless with precipitation of $AgSbF_6$ and $AgSb_2F_{11}$. In addition, during routine preparations of $Ag(SbF_6)_2$ in the last ten years for different purposes,[32,46,47] many times it happened that the isolated dry $Ag(SbF_6)_2$ was not completely sky-blue but its colour varied from greenish-blue to green. It was also observed that, when dry sky-blue $Ag(SbF_6)_2$ was stored for a few months' time in a glovebox (where the temperature might increase up to 303 K) its colour changed to green-blue. The presence of $Ag(SbF_6)_2$ as a major phase in these samples could (beside by its typical colour) be unambiguously determined from its characteristic Raman spectrum.[48] However, all samples, where a shade of green colour was observed, gave Raman spectra with an additional very intense band at 664 cm^{-1} (Fig. S2, ESI†). Analysis of single crystals of this phase solved the mystery showing that the green phase corresponds to a new intermediate compound in the $AgSbF_6/Ag(SbF_6)_2$ system, *i.e.* $Ag_3(SbF_6)_4$.

Moreover, crystallizations of $Ag(SbF_6)_2$ from its aHF solutions resulted sometimes in green crystals of $Ag_3(SbF_6)_4$ and a colorless solid (instead of sky-blue crystals of $Ag(SbF_6)_2$). The Raman spectra of the colorless solid showed a very narrow intense band at 1864 cm^{-1} which is typical of O_2^+ stretching mode of O_2SbF_6.[49] Cationic Ag(II) solvated in aHF is known to be one of the strongest oxidizers known. In aHF acidified with AsF_5, solvated Ag(II) is capable of oxidizing molecular oxygen at 195 K, but at 213 K the products ($O_2AsF_6/AgAsF_6$) re-establish the reactants ($Ag(II)_{(sol)}/O_{2(g)}/AsF_{5(sol)}$).[50] It seems that

in the case of $Ag(SbF_6)_2$, dissolved in aHF, the silver(II) salt is only partly reduced, forming $Ag(I)_2Ag(II)(SbF_6)_4$ and O_2SbF_6 as a by-product. Therefore crystals of $Ag_3(SbF_6)_4$ may also be formed *in situ* during the slow reaction of $Ag(SbF_6)_2$ with traces of water or oxygen penetrating through the walls of crystallization vessels (*cf.* the Experimental part).

Since the chemical identity of the green phase has been established, many attempts were made to synthesize larger quantities of $Ag_3(SbF_6)_4$ as a high-purity product suitable for physicochemical characterization. The most obvious path – by direct reaction between the corresponding amounts of $AgSbF_6$ and $Ag(SbF_6)_2$ in liquid aHF (eqn (1)) – has failed

$$2AgSbF_6 + Ag(SbF_6)_2 \xrightarrow[298\ K]{aHF_{(liq)}} 2xAgSbF_6 + xAg(SbF_6)_2 + (1-x)Ag_3(SbF_6)_4 \quad (1)$$

since instead of the desired pure $Ag_3(SbF_6)_4$, the sample contaminated with the substrates was always obtained. Several other approaches were also tested (see the Experimental section) but either no reaction was observed (i), or mixtures of several products were obtained (ii–v):

(i) $2AgSbF_6 + Ag(SbF_6)_2$ in liquid $SbF_5 \rightarrow$ no reaction;

(ii) $2AgBF_4 + AgF_2$ in liquid SbF_5 and gaseous aHF $\rightarrow$ $AgSb_2F_{11}$ and $Ag_3(SbF_6)_4$;

(iii) $2AgSb_2F_{11} + AgF_2$ in gaseous aHF $\rightarrow$ $AgSbF_6$, $Ag(SbF_6)_2$ and $Ag_3(SbF_6)_4$;

(iv) $Ag(SbF_6)_2 + H_2$ in liquid aHF $\rightarrow$ $AgSbF_6$ and $AgSb_2F_{11}$;

(v) $Ag(SbF_6)_2 + H_2O$ in liquid aHF $\rightarrow$ $AgSbF_6$ and $Ag(SbF_6)_2$.

Finally, it was established that the solid state reaction between $2AgSbF_6$ and $Ag(SbF_6)_2$ at 318 K in the presence of traces of the aHF mediator in the gas phase provides the optimum way to prepare high-purity $Ag_3(SbF_6)_4$ (eqn (2))

$$2AgSbF_6 + Ag(SbF_6)_2 \xrightarrow[318\ K]{aHF_{(g)}} Ag_3(SbF_6)_4 \quad (2)$$

According to quantitative phase analysis based on powder X-ray diffraction, the so-obtained product contains 96.6 wt% $Ag_3(SbF_6)_4$ and 3.4 wt% $AgSbF_6$; $Ag(SbF_6)_2$ could not be detected in the powder pattern. This sample has also proven to be suitable for ESR characterization and hence magnetic measurements were performed since $Ag(SbF_6)_2$ could not be detected in the spectra/magnetization curves (recall $AgSbF_6$ is diamagnetic).

Crystal structures of $Ag_3(SbF_6)_4$ and related $K_2Ag(SbF_6)_4$

The title compound has been found to crystallize in the body-centered cubic cell ($I\bar{4}3d$), with a = 12.3613(4) Å (Table 1). The related potassium compound, green $K(I)_2Ag(II)(SbF_6)_4$, is isomorphic, albeit with a larger unit cell vector of a = 12.498(1) Å, consistent with the larger ionic radius of K(I) than that of Ag(I). There are four formula units inside the unit cell. There is only one Ag atom, one Sb atom and two crystallographically independent F atoms inside the irreducible cell (Fig. 2).

Inspection of the Medea database[15] returns over 500 crystal structures of inorganic compounds containing at least one metal atom, which adopt the $I\bar{4}3d$ space group (no. 220).

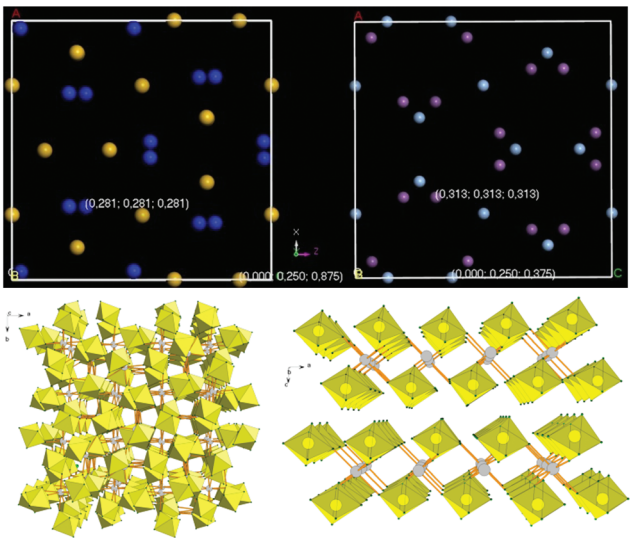

Fig. 2 Top: comparson of the unit cells of the $I\bar{4}3d$ polytype of Si_3N_4 and[51] that of the Ag & Sb sublattice of $Ag(I)_2Ag(II)(SbF_6)_4$. Note the similarity of the N & Sb sublattices. Bottom: the packing diagrams of $Ag(I)_2Ag(II)(SbF_6)_4$ (left) and $Ag(SbF_6)_2$ (right) (grey circles: silver atoms; yellow octahedra: SbF_6 units), two projections were shown.

However, despite their A_3B_4 stoichiometry for many of these compounds, none of them is isostructural to $Ag_3(SbF_6)_4$.[52] In particular, none of the very few quasi-binary $A(I)A(II)_2B_4$ compounds of elements, which are known to exhibit both the first and second oxidation state (Cu, Ag, Au, Hg), adopt the $I\bar{4}3d$ polytype; for example, Cu_3Cl_4 is isomorphic to magnetite (Fe_3O_4, spinel). Similarly, we could not find good structural analogies for $A(II)A(IV)_2B_4$ compounds where B is a divalent anion, such as Pt_3O_4 or Pb_3O_4. However, it turns out that the crystal structure of $Ag_3(SbF_6)_4$ is somewhat similar to that of a certain metastable polytype of Si_3N_4 (Fig. 2).[51]

The Sb/N atom in these structures occupies the (x, x, x) position where $x = \frac{1}{2} + \delta$, with $\delta \approx 0.03$ (N) and $\delta \approx 0.06$ (Sb); for $x = 0$ the packing of anions would correspond to the ideal bcc sublattice. The major difference between both structures is that the Ag atom is found in the (0, 1/4, 3/8) position while the Si atom occupies the (0, 1/4, 7/8) one, which leads to a different bonding pattern. Each compound, however, may be viewed as a defective and severely distorted AB polytype, $[A\square A_3]B_4$.

The most interesting feature of the crystal structure of $Ag_3(SbF_6)_4$ of relevance to its mixed-valence character is that all silver atoms are found in a single crystallographic site (occupying a 12b Wyckoff position at the $\bar{4}$ axis) thus reflecting a random distribution of the Ag(I) and Ag(II) cations (in the 2 : 1 ratio). Thus, irrespective of a noticeable difference in ionic radii of Ag(I) and Ag(II), all silver cations are found in an identical environment of eight fluorine atoms (Fig. 3). Such a feature would imply that $Ag_3(SbF_6)_4$ is in fact an intermediate valence (Class III) system, with an average oxidation state of Ag of $+1\frac{1}{3}$, while rendering $Ag_3(SbF_6)_4$ the first Ag(II)/Ag(I) system of this

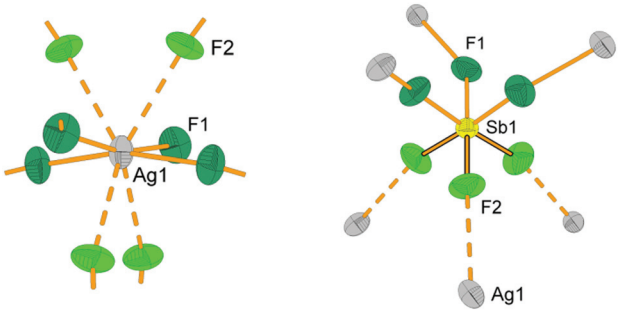

Fig. 3 The 4 + 4 coordination sphere of silver and the closest contacts to the $[SbF_6]^-$ anion in the crystal structure of $Ag_3(SbF_6)_4$ (dashed lines: longer Ag1···F2 contacts; outlined bonds: shorter Sb1–F2 distances; thermal ellipsoids are drawn at the 40% probability level).

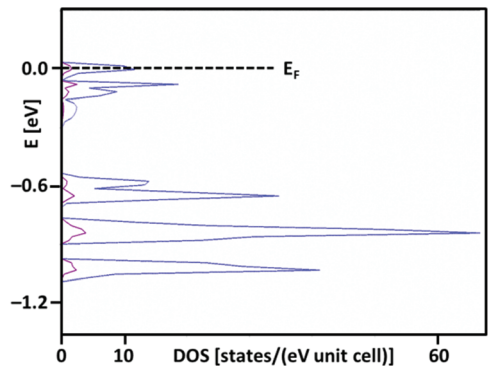

Fig. 4 The electronic density of states of $Ag_3(SbF_6)_4$ calculated while assuming its intermediate-valence (Class III) metallic character (GGA/PBEsol calculation). Partial DOS (contribution from Ag_{4d} – blue and F_{2p} states – mauve) is also shown.

type. What is more, $Ag_3(SbF_6)_4$ would then be analogous to a family of the long known silver clathrate salts Ag_7O_8X (X = NO_3, HF_2, HCO_3, *etc.*) which also crystallize in cubic lattices, and they are comproportionated, metallic and superconducting, with an average oxidation state of silver of +2.43.[53] Indeed, in the case of comproportionation $Ag_3(SbF_6)_4$ would be metallic, with a substantial density of states at the Fermi level (Fig. 4) available for Bose–Einstein condensation, and thus likely even superconducting below a certain temperature.

However, it turns out that the situation for $Ag_3(SbF_6)_4$ is more complex than that. The first coordination sphere of silver consists of four short bonds to fluorine (2.316(7) Å) which are arranged in a close-to square planar geometry, and four additional long contacts at 2.764(6) Å (Fig. 1). The short contacts are too long for typical Ag(II)–F bonds (in $Ag(SbF_6)_2$: 2.095(5)–2.132(4) Å;[34] in $[IF_6][Ag(SbF_6)_3]$: 2.11(1) Å;[32] in $AgFAsF_6$: 1.995(5)–2.004(5) Å;[54] AgF_2: 2.086 Å[55]) and simultaneously too short for Ag(I)–F bonds (the shortest Ag–F bond lengths in $AgBF_4$ are 2.561(4) Å,[56] in $AgSbF_6$ 2.505(2) Å,[57] in $AgSb_2F_{11}$ 2.472(8) Å[33] and in AgF 2.55 Å[58]). Not surprisingly, the valence bond sum analysis[59] suggests that such coordination corresponds to a severely overbonded Ag(I) (VBS = 1.288) and strongly underbonded Ag(II) (VBS = 1.252). This alone is a peculiar but not disqualifying factor, since a silver site should indeed have bonding characteristics typical of $Ag^{+1\frac{1}{3}}$.[60] However, closer inspection of thermal ellipsoids of fluorine atoms next to silver cations reveals an unusual flattened shape, indicating a possibility that F atoms might exhibit static disorder, and thus there might be at least two types of silver cations in the structure, each with a different coordination sphere. One site would have a markedly covalent Ag(II)–F bonding with a nearly square-planar AgF_4 unit, while the other would resemble a typical Ag(I)–F site with eight ligands in a more ionic environment[61] (Fig. 1). This surmise is further supported by the fact that the latter site – corresponding to Ag(I) – may be substituted with K(I) in a new distinct compound, $K_2Ag(SbF_6)_4$ (Table 1).[62]

Based on what was discussed above, one may suspect that – despite a single crystallographic site for Ag in $Ag_3(SbF_6)_4$ – this compound is not a genuine Class III system. However, it is still unclear at this stage whether $Ag_3(SbF_6)_4$ is a well-defined frozen-valence Class I or rather a Class II system. Since vibrational spectra – albeit different for $Ag_3(SbF_6)_4$, $Ag(SbF_6)_2$ and $AgSbF_6$ (*cf.* ESI†) – are not unequivocally indicative of oxidation states, we have further studied $Ag_3(SbF_6)_4$ with a range of physicochemical methods more sensitive to the nature of silver cations present in this compound.

X-ray absorption near-edge structure spectroscopy (XANES) of $Ag_3(SbF_6)_4$ and Ag(I)SbF_6, and $IF_6[Ag(II)(SbF_6)_3]$ references

The average value of the Ag oxidation state in the $Ag_3(SbF_6)_4$ sample was obtained by Ag K-edge XANES analysis. The binding energies of the valence orbitals and therefore the energy position of the edge and the pre-edge features in the XANES spectrum are known to be correlated with the valence state of the absorbing atom in the sample. Namely, each absorption feature in the XANES spectrum is shifted to higher energies with an increasing oxidation state of a given element; this feature is now routinely used to deduce the valence state.[42,43,63,64] For example, examining the XANES spectra of two reference compounds $AgSbF_6$[65] and $IF_6[Ag(SbF_6)_3]$[32] (Fig. 5) with a known crystal structure and a Ag valence state, we found out that the Ag K-edge shifts by about 5.4 eV per valence from Ag(I) to Ag(II).

If the sample contains the same element in two or more sites with a different local structure and/or valence state, the measured XANES spectrum is a linear combination of individual XANES spectra of individual sites. In such a case the relative amounts of cations at each site can be determined by the linear combination fit using XANES spectra of appropriate reference compounds, *i.e.* compounds that contain the element with the same valence state and the same or very similar local structure to the element on each site in the sample.[43,63,64] We applied this procedure to the Ag XANES spectrum measured for the $Ag_3(SbF_6)_4$ sample. The spectrum may indeed be described as a linear combination of the

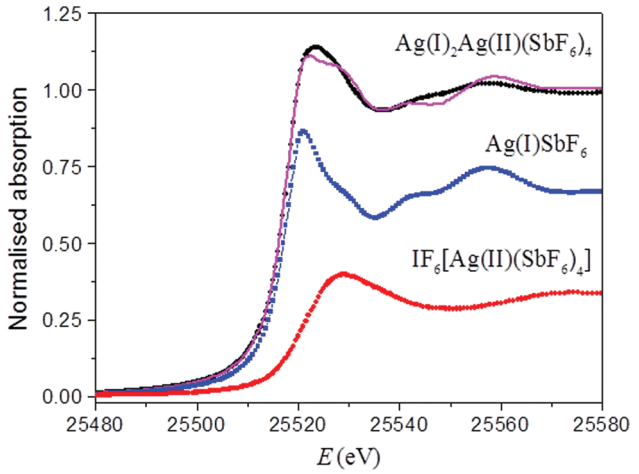

Fig. 5 The Ag K-edge XANES spectrum of a $Ag_3(SbF_6)_4$ (black dots) and best-fit linear combination (magenta line) of XANES profiles of Ag(I)SbF_6 (blue line) as a reference for Ag(I) and $IF_6[Ag(II)(SbF_6)_3]$ (red line) as a reference for Ag(II), with the relative weight of 68% and 32%, respectively.

XANES profiles of $AgSbF_6$ (containing Ag(I) in the 8-coordinated site) and $IF_6[Ag(SbF_6)_3]$ (containing Ag(II) in a close-to square-planar site) (Fig. 5). The fit yields the relative amounts of Ag(I) and Ag(II) of, respectively, 68% and 32%, with an uncertainty of about 2%; obtained values are in excellent agreement with the expected ones of 66.6% and 33.3% for the proposed structure of the sample.

Thus, XANES results have nicely confirmed not only the average oxidation state of silver ($+1\frac{1}{3}$) in $Ag_3(SbF_6)_4$, but also that the Ag cations in the structure are present in two valence states Ag(I) and Ag(II) in a relative ratio of 2 to 1.

ESR spectra and magnetochemistry of $Ag_3(SbF_6)_4$ and $Ag(SbF_6)_2$

One of the key features which distinguish Ag(II) from Ag(I) – apart from voracious oxidizing properties of Ag(II) – is the presence of one unpaired electron in the former species ($4d^9$), while the latter is diamagnetic ($4d^{10}$). This allows easy detection of the presence of paramagnetic Ag(II) in the samples by applying electron spin spectroscopy and magnetometry.

The ESR spectrum of the $Ag(II)(SbF_6)_2$ reference sample taken at room temperature (Fig. 6) shows the presence of a familiar two-constituent signal with the following components of the g tensor: $g_{\|} = 2.699$ and $g_{\perp} = 2.161$. When the temperature is decreased to 120 K, the higher-field signal is split into two, with $g_{\|} = 2.702$, $g_{\perp 1} = 2.149$, and $g_{\perp 2} = 2.103$. Such components of the rhombic g tensor with $g_{\|} \gg g_{\perp 1} \approx g_{\perp 2}$ suggest that the local environment of Ag(II) takes the slightly distorted square-planar form (*i.e.* a strongly elongated octahedron)[66–68] consistent with the previously determined crystal structure of this compound (Fig. 2).[34] The absolute values of the g tensor components are larger than the corresponding values for

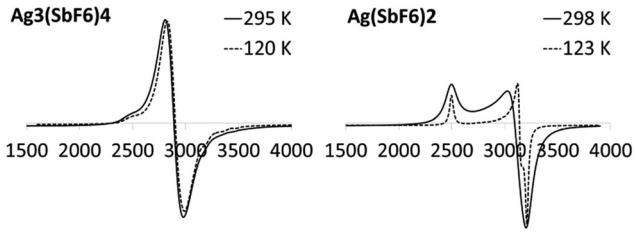

Fig. 6 The ESR spectra (X-band) of $Ag_3(SbF_6)_4$ and Ag(II)SbF_6.

$AgZrF_6$ ($g_{\|} = 2.58$, $g_{\perp} = 2.11$) and $AgSnF_6$ ($g_{\|} = 2.65$, $g_{\perp} = 2.12$)[66] in agreement with the weaker ligand field[66,69] exerted by weakly coordinating SbF_6^- anions than those of the more electron-rich MF_6^{-2} ones (M = Zr, Sn).

On the other hand, the ESR spectrum of $Ag_3(SbF_6)_4$ recorded at room temperature (Fig. 6) shows the presence of a broad signal at $g = 2.333$, with some weak additional features. When the temperature is decreased to 120 K, the signal shifts slightly to $g = 2.324$ but without splitting. The measured g value is similar to the arithmetic average of $g_{\|}$, $g_{\perp 1}$, and $g_{\perp 2}$ obtained for $Ag(SbF_6)_2$, *i.e.* 2.318 (at 120 K). This result clearly suggests that (i) distinct paramagnetic Ag(II) cations are present in the crystal structure of $Ag_3(SbF_6)_4$ while (ii) the local environment of Ag(II) possibly takes the form of a square plane albeit either substantial local disorder or/and fast relaxation, which broadens the signal and prevents the separation of g components.

The magnetic susceptibility of $Ag_3(SbF_6)_4$ has been investigated between 2 K and 300 K in a constant magnetic field H = 1000 Oe. The molar magnetic susceptibility free from diamagnetic core contribution[70] as a function of temperature of $Ag_3(SbF_6)_4$ is plotted in Fig. 7. The susceptibility monotonically increases with decreasing temperature and obeys a Curie–

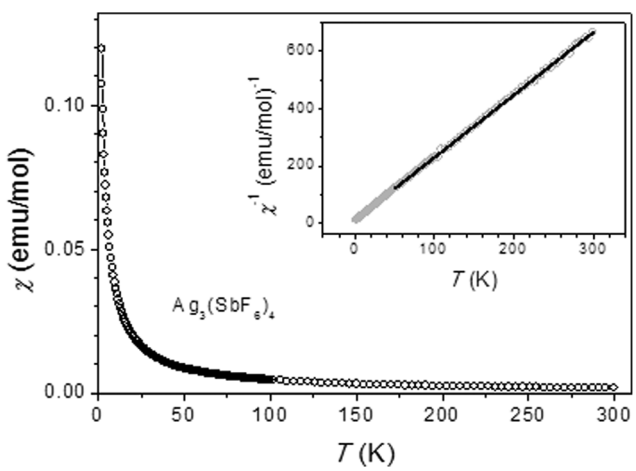

Fig. 7 Temperature-dependent susceptibility $\chi(T)$ and inverse susceptibility $\chi^{-1}(T)$ (inset) of $Ag_3(SbF_6)_4$ as measured in a magnetic field H = 1000 Oe. The full line in the inset is a fit with the Curie–Weiss law.

Weiss law as can be observed from linear χ^{-1} *vs.* T dependence (inset in Fig. 7). In the 50–300 K temperature range the data were fitted to the Curie–Weiss law with the Curie constant C = 0.46 emu K mol^{-1} (μ_{eff} = 1.9 B.M.) and θ_p = −4.0 K. The value of the Curie constant is consistent with the spin-only value for one Ag(II) per formula unit. This result further confirms that one out of three silver cations corresponds to paramagnetic Ag(II) while the remaining two cations are diamagnetic Ag(I). The negative value of θ_p is characteristic of weak antiferromagnetic interactions. Further comparison of magnetic properties of $Ag_3(SbF_6)_4$ with those of parent $Ag(SbF_6)_2$ is given in ESI.†

Concluding this section we note that ESR spectroscopy as well as magnetometry have helped to unequivocally establish $Ag_3(SbF_6)_4$ as a mixed-valence (Class I) compound with localized oxidation states, *i.e.* $Ag(I)_2Ag(II)(SbF_6)_4$, and despite the same crystallographic site occupied by both types of cations.

Electronic spectra of $Ag_3(SbF_6)_4$, $Ag(SbF_6)_2$, and $AgSbF_6$ in the UV-vis-NIR range

Electronic spectra – in conjecture with the ESR spectra and quantum mechanical calculations – have proven in the past to be very useful for analysis of chemical bonding in the Ag(II) systems.[66–69] Here we have studied the electronic spectra for the samples of $Ag_3(SbF_6)_4$, and two reference samples ($Ag(SbF_6)_2$ and $AgSbF_6$) in the NUV-vis-NIR range (5–50k cm^{-1} or *ca.* 0.6–6.2 eV).

The reflectance spectra in the vis-NIR region are presented in Fig. 8, while the less informative NUV region is shown in ESI.†

The spectrum of $Ag(SbF_6)_2$ is rich in bands (I–VI in Fig. 8). Since local geometry at the Ag(II) site in this compound is quasi-tetragonal, the assignment is based on the literature data for related compounds of Ag(II) exhibiting D_{4h} local symmetry.[66–69] The broad band centered at 9.95k cm^{-1} (I) is assigned to the $5a_{1g}\rightarrow 3b_{1g}$ transition, that at 13.64k cm^{-1} (II) to the $2b_{2g}\rightarrow 3b_{1g}$, while the one at 17.83k cm^{-1} (III) to the $3e_g\rightarrow 3b_{1g}$. From these energies of d–d transitions one may immediately derive[66] the values δ_1 and δ_2 governing the splitting of the, respectively, ^2E_g and $^2T_{2g}$ terms, as follows: δ_1 = 2.49k cm^{-1} and δ_2 = 1.40k cm^{-1}, as well as the value of the ligand-field splitting energy, Δ = 11.45k cm^{-1}. The value of Δ falls in the 9.2–12.0k cm^{-1} range typical of compounds of Ag(II).[66]

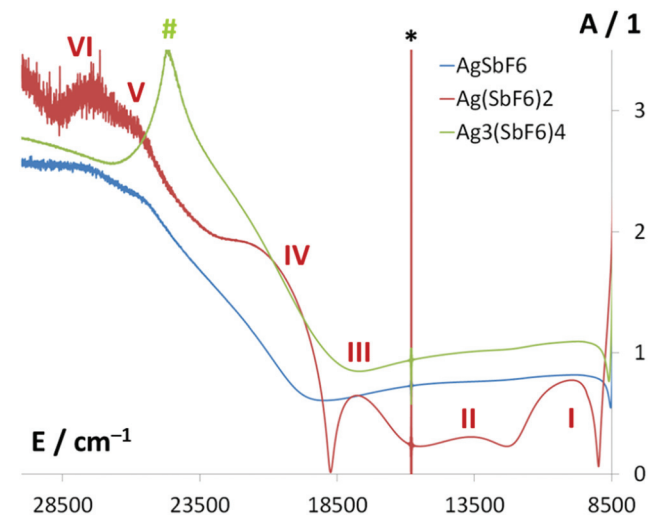

Fig. 8 Electronic absorption spectra of $Ag_3(SbF_6)_4$, $Ag(SbF_6)_2$, and $AgSbF_6$ in the vis-NIR region. The 5–8.5k cm^{-1} region is predominated by instrumental artefacts and it has not been shown. Starlet marks the artefact, while Roman numbers and # indicate bands which are discussed in the text.

The broad absorption seen at *ca.* 20–21.5k cm^{-1} (IV) has not been assigned in the past; judging from its energy and using the previously computed orbital scheme[67,69] and selection rules, we tentatively assign it to the charge-transfer (CT) transition $2e_g\rightarrow 3b_{1g}$ involving axial F atoms, $F_{ax}\rightarrow Ag(II)$. Using the same scheme, the absorption seen at *ca.* 25.9–27.6k cm^{-1} (V–VI) may be assigned to another $F_{ax}\rightarrow Ag(II)$ CT transition ($4a_{1g}\rightarrow 3b_{1g}$) which is split since local symmetry around Ag(II) is in fact slightly departing from ideal D_{4h} (equatorial Ag–F bond lengths are 2.09 Å and 2.13 Å). The CT transitions involving equatorial F atoms, $F_{eq.}\rightarrow Ag(II)$, have been predicted[67,69] to fall in the region 35–41k cm^{-1} and, indeed, some absorption is seen in this part of the NUV region (ESI†).

The electronic spectrum of $Ag_3(SbF_6)_4$ is rather poor in bands as compared to that of $Ag(SbF_6)_2$. The bands I–III are hard to detect, which likely originates from substantial static disorder of F atoms around Ag(II) in this compound, and thus to excessively broad absorption bands. An unstructured shoulder may be seen at *ca.* 21.3k cm^{-1} possibly corresponding to the CT transition analogous to IV seen for $Ag(SbF_6)_2$. The strong band (#) peaking at 24.67k cm^{-1} (3.06 eV, 405 nm) is the only preeminent feature of the absorption spectrum. Such a strong feature is absent in the spectrum of $Ag(SbF_6)_2$ and also the $AgSbF_6$ reference. Since mixed-valence compounds often exhibit a new strong electronic absorption band due to the inter-valence charge transfer (IVCT) transition, it is tempting to assign the 405 nm absorption band to the vertical $Ag(I)\rightarrow Ag(II)$ CT process. The energy of this transition is quite large (3 times larger than that of the d–d transitions) and thus the valences are firmly localized in $Ag_3(SbF_6)_4$, while the electronic conduction due to electron hopping between Ag(I) and Ag(II) sites must be difficult. Indeed, single crystals of $Ag_3(SbF_6)_4$ are quite transparent to light and they do not exhibit metallic luster, typical of metals and narrow-band gap semiconductors.

Conclusions and prospect

We have prepared and studied $Ag_3(SbF_6)_4$, which is one of five currently known mixed-valence compounds of Ag(II)/Ag(I). This compound crystallizes in the cubic system ($I\bar{4}3d$ cell) with just one crystallographic position for silver cations, which finds no precedence in the chemistry of Ag(II)/Ag(I) compounds of

silver. A number of physicochemical methods applied have confirmed the mixed- (Class I) and not an intermediate-valence (Class III) character of this compound. The localized-oxidation state character, *i.e.* $Ag(I)_2Ag(II)(SbF_6)_4$, cannot be deduced from X-ray data due to substantial static disorder of fluorine atoms of the SbF_6^- anions, which leads to a misleading averaged bonding picture. The strong absorption band seen at 3.05 eV in the electronic spectrum of $Ag_3(SbF_6)_4$ has been tentatively assigned to the IVCT transition, Ag(I)→Ag(II). If the energy of this transition were substantially decreased due to application of a large external pressure,[71] a fraction of Ag(4d) electrons should become itinerant thus resulting in metallic conductivity, like it has been observed for other prototypical mixed-valence systems.

Since $Ag_3(SbF_6)_4$ may be obtained from $2AgSbF_6 + Ag(SbF_6)_2$ precursors, it seems the enthalpy factor is slightly in favour of the formation reaction; this process may be viewed as a Lewis acid/Lewis base reaction, with $Ag(SbF_6)_2$ playing the role of an acid, similar to the analogous case of $Ag_3(SO_3F)_4$ formation. Moreover, the volume of $Ag_3(SbF_6)_4$ per formula unit (~472.21 Å^3) is slightly larger than that of the reactant mixture (~454.93 Å^3) which points to an additional small entropic stabilization of $Ag_3(SbF_6)_4$ (of about 9.2 kJ mol^{-1} in ST factor) with respect to the substrates.[72] The quest for new mixed-valence compounds of Ag(II)/Ag(I) – and in particular the Class III systems – is on.

Acknowledgements

Z.M., E.G., Z.J. and I.A. gratefully acknowledge the Slovenian Research Agency (ARRS) for the financial support of the present study within the research program: P1-0045 Inorganic Chemistry and Technology, P1-0112 Studies of atoms, molecules and structures with photons and particles, and P2-0348 New imaging and analytic methods. The project 'AgCENT: novel unique magnetic and electronic materials based on Ag(II) compounds' is financed by the Polish National Science Centre (NCN, project UMO-2011/01/B/ST5/06673). The selected measurements were carried out by using the CePT infrastructure financed by the EU European Regional Development Fund within the Operational Programme "Innovative economy" for 2007–2013 (POIG.02.02.00-14-024/08-00). DFT calculations were carried out using ICM supercomputers (grant G29-3). Access to beamline BM23 of European Synchrotron Radiation Facility within the project LS 2209 is acknowledged. We would like to thank Gleb Parakhonskiy and Olivier Mathon of ESRF for expert advice on beamline operation.

References

1 P. Day, N. S. Hush and J. H. Clark, *Philos. Trans. R. Soc. London, Ser. A*, 2008, **366**, 5–14.
2 J. P. Fackler Jr., Mixed Valence Compounds, in *Encyclopedia of Inorganic Chemistry*, ed. R. B. King, John Wiley & Sons, Chichester, 2005, vol. 5.
3 K. D. Demadis, C. M. Hartshorn and T. J. Meyer, *Chem. Rev.*, 2001, **101**, 2655–2685.
4 J. Woodward, *Philos. Trans. R. Soc. London*, 1724, **33**, 15. The first synthesis, however, took place in 1704.
5 M. B. Robin and P. Day, *Adv. Inorg. Chem. Radiochem.*, 1967, **10**, 248–422.
6 G. C. Allen and N. S. Hush, in *Progress in Inorganic Chemistry*, John Wiley & Sons, New York, 1967, vol. 8, pp. 357–389.
7 C. Creutz and H. Taube, *J. Am. Chem. Soc.*, 1973, **95**, 1086–1094.
8 R. A. Marcus, *J. Chem. Phys.*, 1956, **24**, 966–978.
9 J. G. Bednorz and K. A. Müller, *Z. Phys. B: Condens. Matter*, 1986, **64**, 189–193.
10 Y. Tokura, H. Takagi and S. Uchida, *Nature*, 1989, **337**, 345–347.
11 E. Dagotto, *Rev. Mod. Phys.*, 1994, **66**, 763–840.
12 K. J. Fijałkowski and W. Grochala, *Dalton Trans.*, 2008, 5447–5453.
13 C. H. Ahn, *et al.*, *Rev. Mod. Phys.*, 2006, **78**, 1185–1212.
14 A. T. Bollinger, G. Dubuis, J. Yoon, D. Pavuna, J. Misewich and I. Božović, *Nature*, 2011, **472**, 458–460.
15 The Infomatica 3.1 database of Medea package lists over 4.1 thousand structures of quaternary (4-element) copper oxides $A_tB_xCu_yO_z$ (excluding systems such as complex sulphates, nitrates *etc.*), over 3.0 thousand systems built of 5 elements, over 1.3 thousand combinations of 6 and more-elements. © Materials Design (2014).
16 These attempts left rather little trace in the literature, since failed experiments are less frequently reported than the successful ones. J. Wang and M. Sayer, *Cryogenics*, 1993, **33**, 1164–1169; A. K. Tyagi, S. Tyagi and T. P. Sharma, *Mater. Sci. Eng., B*, 1997, **45**, 88–97; J. E. Rodriguez, A. Marino and J. Giraldo, *Physica C*, 1997, **282**, 1253–1254.
17 W. Grochala and R. Hoffmann, *Angew. Chem., Int. Ed.*, 2001, **40**, 2742–2781.
18 K. Yvon, A. Bezinge, P. Tissot, *et al.*, *J. Solid State Chem.*, 1986, **65**, 225–230.
19 M. Jansen and P. Fischer, *J. Less-Common Met.*, 1988, **137**, 123–131.
20 W. Grochala, *Scr. Mater.*, 2006, **55**, 811–814.
21 X. Yang and H. Su, *Sci. Rep.*, 2014, **4**, 5420.
22 W. Grochala, *J. Mater. Chem.*, 2009, **19**, 6949–6968.
23 W. Grochala, *J. Mol. Model*, 2011, **17**, 2237–2248.
24 Q.-M. Wang, H. K. Lee and T. C. W. Mak, *New J. Chem.*, 2002, **26**, 513–515.
25 Q.-M. Wang and T. C. W. Mak, *Chem. Commun.*, 2001, 807–808.
26 A system erroneously claimed to contain Ag(II) and Ag(I) has been later shown to be a Ag(I) system (the presence of H^+ escaped the attention of the first set of researchers): D. Sun, C.-F. Yang, H.-R. Xu, H.-X. Zhao, Z.-H. Wei,

N. Zhang, L.-J. Yu, R.-B. Huang and L.-S. Zheng, *Chem. Commun.*, 2010, 8168–8170; P. J. Leszczyński, A. Budzianowski, M. Derzsi, Ł. Dobrzycki, M. K. Cyrański and W. Grochala, *Dalton Trans.*, 2012, **41**, 396–402.

27 P. C. Leung and F. Aubke, *Inorg. Chem.*, 1978, **17**, 1765–1772.

28 T. Michałowski, P. Malinowski, M. Derzsi, Z. Mazej, Z. Jagličić, P. J. Leszczyński and W. Grochala, *Eur. J. Inorg. Chem.*, 2011, 2508–2516.

29 T. Michałowski *et al.*, 16th Frühjahrssymposium of the Münster Division of the German Chemical Society's Young Chemists Section, Münster 26–29.03.2014.

30 P. J. Malinowski *et al.*, manuscript in preparation, 2015.

31 D. Grzybowska, P. Malinowski, Z. Mazej and W. Grochala, *Collect. Czech. Chem. Commun.*, 2008, **73**, 1729–1746.

32 Z. Mazej, E. Goreshnik, I. Arčon, N. Zabukovec Logar and V. Kaučič, *Z. Anorg. Allg. Chem.*, 2010, **636**, 224–229.

33 Z. Mazej and P. Benkič, *Inorg. Chem.*, 2003, **42**, 8337–8343.

34 D. Gantar, I. Leban, B. Frlec and J. H. Holloway, *J. Chem. Soc., Dalton Trans.*, 1987, 2379–2383.

35 A. Altomare, M. Cascarano, C. Giacovazzo and A. Guagliardi, *J. Appl. Crystallogr.*, 1993, **26**, 343–350.

36 Molecular Structure Corporation, *teXsan for Windows. Single Crystal Structure Analysis Software. Version 1.06*, MSC, 9009 New Trails Drive, The Woodlands, TX 77381, USA, 1997–1999.

37 L. J. Farrugia, *J. Appl. Crystallogr.*, 1999, **32**, 837–838.

38 G. M. Sheldrick, *Acta Crystallogr., Sect. A: Fundam. Crystallogr.*, 2008, **64**, 112–122.

39 *DIAMOND v3.1*, Crystal Impact GbR, Bonn, Germany, 2004–2005.

40 *Materials Studio v.8.0.0.843*, © Dassault Systems, 2014.

41 B. Ravel and M. Newville, *J. Synchrotron Radiat.*, 2005, **12**, 537–541.

42 J. Wong, F. W. Lytle, R. P. Messmer and D. H. Maylotte, *Phys. Rev. B: Condens. Matter*, 1984, **30**, 5596–5610.

43 P. Behrens, S. Assmann, U. Bilow, C. Linke and M. Jansen, *Z. Anorg. Allg. Chem.*, 1999, **625**, 111–116.

44 I. Ahmed, E. A. Abou Neel, S. P. Valappil, S. N. Nazhat, D. M. Pickup, D. Carta, D. L. Carroll, R. J. Newport, M. E. Smith and J. C. Knowles, *J. Mater. Sci.*, 2007, **42**, 9827–9835.

45 G. Kresse and J. Furthmüller, *Phys. Rev. B: Condens. Matter*, 1996, **54**, 11169–11186; G. Kresse and D. Joubert, *Phys. Rev. B: Condens. Matter*, 1999, **59**, 1758–1775.

46 P. J. Malinowski, M. Derzsi, Z. Mazej, Z. Jaglčić, B. Gaweł, W. Łasocha and W. Grochala, *Angew. Chem., Int. Ed.*, 2010, **49**, 1683–1686.

47 P. J. Malinowski, M. Derzsi, Z. Mazej, Z. Jagličić, P. J. Leszczyński, T. Michałowski and W. Grochala, *Eur. J. Inorg. Chem.*, 2011, 2499–2507.

48 Z. Mazej, *J. Fluorine Chem.*, 2004, **125**, 1723–1733.

49 Z. Mazej, M. Ponikvar-Svet, J. F. Liebman, J. Passmore and H. D. B. Jenkins, *J. Fluorine Chem.*, 2009, **130**, 788–791.

50 G. Lucier, C. Shen, W. J. Casteel Jr., L. Chacón and N. Bartlett, *J. Fluorine Chem.*, 1995, **72**, 157–163.

51 M. Billy, J. C. Labbe, A. Selvaraj and G. Roult, *Mater. Res. Bull.*, 1983, **18**, 921–934; P. Kroll, *J. Solid State Chem.*, 2003, **176**, 530–537.

52 The most frequently found types are those similar to stoichiometric $Th(IV)_3(As^{3-})_4$ ($Z = 4$), $Bi(III)_4(SiO_4)_3$ ($Z = 4$) or to (formally) mixed valence $Pr(II)Pr(III)_2(S^{2-})_4$ ($Z = 4$).

53 I. Naray-Szabo, G. Argay and P. Szabo, *Acta Crystallogr.*, 1965, **19**, 180; M. B. Robin, K. Andres, T. H. Geballe, N. A. Kuebler and D. B. McWhan, *Phys. Rev. Lett.*, 1966, **17**, 917–919; M. Jansen and S. Vensky, *Z. Naturforsch., B: Anorg. Chem. Org. Chem.*, 2000, **55**, 882–886.

54 D. Gantar, B. Frlec, D. R. Russell and J. H. Holloway, *Acta Crystallogr., Sect. C: Cryst. Struct. Commun.*, 1987, **43**, 618–620.

55 A. Jesih, K. Lutar, B. Žemva, B. Bachmann, S. Becker, B. G. Müller and R. Hoppe, *Z. Anorg. Allg. Chem.*, 1990, **588**, 77–83.

56 E. Goreshnik and Z. Mazej, *Solid State Sci.*, 2005, **7**, 1225–1229.

57 K. Matsumoto, R. Hagiwara, Y. Ito and O. Tamada, *J. Fluorine Chem.*, 2001, **110**, 117–122.

58 P. M. Halleck, J. C. Jamieson and C. W. F. T. Pistorius, *J. Phys. Chem. Solids*, 1972, **33**, 769–773; B. G. Müller, *Angew. Chem., Int. Ed. Engl.*, 1987, **26**, 1081–1097.

59 Analysis performed using parameters listed in: http://www.ccp14.ac.uk/ccp/web-mirrors/i_d_brown/, *i.e.* $R_{Ag(I)} = 1.8$ Å, $R_{Ag(II)} = 1.79$ Å and $s = 0.37$.

60 The Sb–F2 distances are quite short (1.839(6) Å) and in the range of typical Sb–F_t (F_t = terminal fluorine atom) distances. Since antimony atom occupies a 16c Wyckoff position at the 3 axis, according to the symmetry, each SbF_6 unit has three such short Sb–F2 distances. The coordination sphere of each Sb atom is completed by additional three fluorine atoms at much longer distances (1.886(7) Å), typical of Sb–F_b contacts (F_b = bridging fluorine atom). Indeed, F1 acts as a linker atom in the Sb–F1–Ag bridges. Similar Sb–F bond lengths were observed for $Ag(SbF_6)_2$ [52] where three fluorine atoms play a bridging role, and three others are terminal.

61 As seen *e.g.* for $AgBF_4$, $AgSb_2F_{11}$ and the high-pressure form of AgF at $p > 2.5$ GPa.

62 Although the quality of X-ray data collected for $K_2Ag(SbF_6)_4$ is not as satisfactory as for $Ag_3(SbF_6)_4$, similar features may be observed in the crystal structure of both compounds. First, there is a random distribution of the K(I) and Ag(II) cations in a 2 : 1 ratio at the same crystallographic positions. Second, there are four short (4 × 2.34(2) Å) and four long K/Ag–F distances (2.82(2) Å); these K/Ag–F distances are too long for Ag(II)–F and too short for typical K–F bonds. Similar to the case of $Ag_3(SbF_6)_4$, this could be explained by abnormal flattened thermal ellipsoids of fluorine atoms, indicating that potassium and silver atoms in fact do not have identical coordination spheres, which is obviously to be expected.

63 R. Dominko, C. Sirisopanaporn, C. Masquelier, D. Hanzel, I. Arčon and M. Gaberšček, *J. Electrochem. Soc.*, 2010, **157**, A1309–A1316.
64 I. Arčon, J. Kolar, A. Kodre, D. Hanžel and M. Strlič, *X-Ray Spectrom.*, 2007, **36**, 199–205.
65 Z. Mazej and R. Hagiwara, *J. Fluorine Chem.*, 2007, **128**, 423–437.
66 C. Friebel and D. Reinen, *Z. Anorg. Allg. Chem.*, 1975, **413**, 51–60.
67 J. A. Aramburu, M. Moreno and M. T. Barriuso, *J. Phys.: Condens. Matter*, 1992, **4**, 9089–9112.
68 A. Monnier, A. Gerber and H. Bill, *J. Chem. Phys.*, 1991, **94**, 5891–5896.
69 R. Valiente, J. A. Aramburu, M. T. Barriuso and M. Moreno, *J. Phys.: Condens. Matter*, 1994, **6**, 4515–4525.
70 O. Khan, *Molecular Magnetism*, VCH Publishers, New York, 1993.
71 W. Grochala, J. Feng, R. Hoffmann and N. W. Ashcroft, *Angew. Chem., Int. Ed.*, 2007, **46**, 3620–3642.
72 H. D. B. Jenkins and L. Glasser, *Inorg. Chem.*, 2003, **42**, 8702–8708.